# Stress and aging induce distinct polyQ protein aggregation states

Lorenza E. Moronetti Mazzeo[a], Devin Dersh[a,b], Marco Boccitto[c,d], Robert G. Kalb[c,d], and Todd Lamitina[a,b,d,1]

[a]Department of Physiology, Perelman School of Medicine, [b]Graduate Group in Biochemistry and Molecular Biophysics, and [d]Neuroscience Graduate Group, University of Pennsylvania, Philadelphia, PA 19104; and [c]Department of Pediatrics, Division of Neurology, Children's Hospital of Philadelphia, Philadelphia, PA 19104

Edited by Gregory A. Petsko, Brandeis University, Waltham, MA, and approved May 3, 2012 (received for review June 3, 2011)

**Many age-related diseases are known to elicit protein misfolding and aggregation. Whereas environmental stressors, such as temperature, oxidative stress, and osmotic stress, can also damage proteins, it is not known whether aging and the environment impact protein folding in the same or different ways. Using polyQ reporters of protein folding in both *Caenorhabditis elegans* and mammalian cell culture, we show that osmotic stress, but not other proteotoxic stressors, induces rapid (minutes) cytoplasmic polyQ aggregation. Osmotic stress-induced polyQ aggregates could be distinguished from aging-induced polyQ aggregates based on morphological, biophysical, cell biological, and biochemical criteria, suggesting that they are a unique misfolded-protein species. The insulin-like growth factor signaling mutant *daf-2*, which inhibits age-induced polyQ aggregation and protects *C. elegans* from stress, did not prevent the formation of stress-induced polyQ aggregates. However, osmotic stress resistance mutants, which genetically activate the osmotic stress response, strongly inhibited the formation of osmotic polyQ aggregates. Our findings show that in vivo, the same protein can adopt distinct aggregation states depending on the initiating stressor and that stress and aging impact the proteome in related but distinct ways.**

protein homeostasis | polyglutamine | Huntington disease | osmoregulation

Organisms operate in a constantly changing environment, and their survival depends on their ability to adjust cellular physiology to adapt to new demands. The environment is known to impact many cellular processes, including the efficiency of protein folding. The process of adjusting the cellular protein-folding environment to match folding demands caused by environmental, physiological, or genetic stressors is termed "protein homeostasis." Environmental stressors can alter protein homeostasis in several different ways. For example, heat shock and oxidative stress cause denaturation and misfolding of proteins via thermal disruption of free energy states and oxidation/glutathione conjugation of oxidized proteins, respectively (1–3). Changes in environmental osmolarity can also lead to disruption of protein folding through undetermined mechanisms (4, 5). Cells respond to these proteotoxic stressors through the activation of specific physiological response pathways that act to increase the abundance or activity of molecules that improve protein folding, such as protein or chemical chaperones (6, 7).

In addition to environmental stress, aging also results in disruptions in protein homeostasis. Although this is a feature of normal physiological aging, it is also observed in several pathological states. For example, in some age-associated neurodegenerative diseases, expanded CAG-repeat mRNAs give rise to unstable polyglutamine (polyQ)-repeat–containing proteins that self-assemble into proteotoxic protein aggregates (8). Proteins containing Q repeats above pathological thresholds of 30–40 place an excessive burden on cellular protein homeostasis systems, leading to age-dependent protein aggregation and cellular toxicity (9). PolyQ-GFP proteins have been used as fluorescent probes to understand the biochemical, biophysical, and genetic aspects of protein aggregation. In addition, polyQ reporters also serve as more general probes of the cellular protein-folding landscape in wide-ranging cellular and organismal contexts (10–14). Although most studies have used these polyQ substrates to investigate the relationship between protein folding and aging, the interactions between the environment and protein folding under in vivo conditions has only recently begun to be explored (4, 5).

*Caenorhabditis elegans* has emerged as a powerful model system for the in vivo study of stress-response pathways and mechanisms of protein folding. Worms exhibit robust, cell-specific, and nonoverlapping transcriptional responses to environmental stressors such as heat shock, oxidative stress, and osmotic stress (15–17). Expression of protein-folding "sensors," such as polyQ proteins, gives rise to the formation of protein aggregation species that can be monitored in live animals (11, 18). Aging pathways influence the age-onset aggregation and toxicity of polyQ and other protein-folding sensors (11, 13, 19–23). Although aging and stress-response pathways are linked (24–27), it is not clear whether environmental stressors and aging affect protein folding and aggregation in similar or distinct ways.

Previous data showed that inhibition of protein homeostasis pathways limits survival of *C. elegans* in hyperosmotic environments (5) and activates osmosensitive gene expression without activating other stress-response pathways (28), suggesting that osmotic stress disrupts protein folding in a stress-specific manner. Indeed, recent studies in *C. elegans* show that both osmotic stress and aging enhance the misfolding of numerous cellular proteins (4, 23). However, the relationship between aging-induced and stress-induced protein misfolding has not been explored. Here we show that in both *C. elegans* and mammalian cells, osmotic stress, but not other stressors, induces the formation of polyQ aggregates that are distinct from aging-induced aggregates. Our findings suggest that stress and aging impact protein folding in distinct ways and that the same protein can adopt unique aggregation states in response to different physiological conditions.

## Results

**Hyperosmotic Stress, but Not Other Stressors, Induces PolyQ Aggregation in the *C. elegans* Intestinal Epithelium.** PolyQ proteins are widely used as sensors to investigate dynamic aspects of age-related protein folding in vivo (13, 20, 22, 23, 29). To investigate how the environment affects protein folding in a live-animal setting, we tested the effects of diverse stressors on an epithelial cell model of polyQ aggregation in the nematode *C. elegans* (18). We used worms containing an integrated transgene [derived from a previously constructed strain (18); *SI Materials and Methods*] that expresses a Q44-YFP protein under the control of the intestine-specific *vha-6* promoter. Exposure of young adult Q44-YFP worms to hyperosmotic stress (500 mM NaCl) caused irreversible and rapid ($\tau_{1/2}$ = 48 ± 4 min)

Author contributions: L.E.M.M., D.D., M.B., R.G.K., and T.L. designed research; L.E.M.M., D.D., M.B., R.G.K., and T.L. performed research; L.E.M.M., D.D., M.B., R.G.K., and T.L. analyzed data; and L.E.M.M., R.G.K., and T.L. wrote the paper.

The authors declare no conflict of interest.

This article is a PNAS Direct Submission.

[1]To whom correspondence should be addressed. E-mail: lamitina@mail.med.upenn.edu.

This article contains supporting information online at www.pnas.org/lookup/suppl/doi:10.1073/pnas.1108766109/-/DCSupplemental.

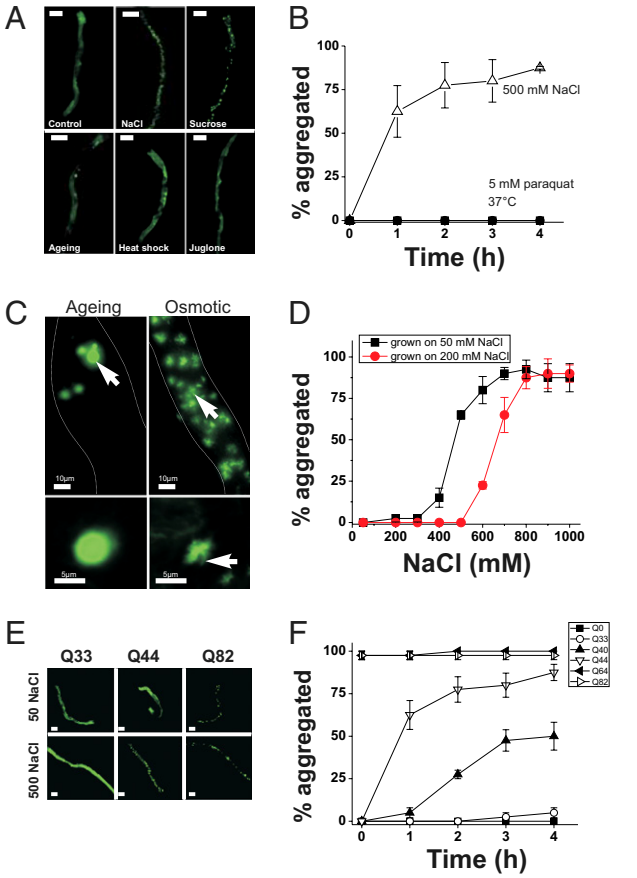


**Fig. 1.** Osmotic stress results in the rapid aggregation of intestinally expressed polyQ proteins at the threshold for activation. (*A*) Q44-YFP localization in the intestine of young adult animals following a 4-h exposure to 50 mM NaCl (Control), 500 mM NaCl, 1 M sucrose, day 3–4 post-L4 stage adult (Aging), 37 °C (Heat shock), or 1 mM juglone. (Scale bars, 100 μm.) (*B*) Quantification of the percentage of animals with >10 Q44 aggregates over time following exposure to the indicated stressor. $n > 40$ animals per condition. Data shown are mean ± SD. (*C*) (*Upper*) Collapsed Z stack of images taken through the entire intestine. Dashed lines indicate intestinal boundary. Arrows point to aging aggregates (*Left*) or osmotic aggregates (*Right*). (*Lower*) Single z-plane image from a deconvolved image series from an aging-induced aggregate (*Left*) or an osmotically induced aggregate (*Right*). The arrow indicates a fibrillar extension that emanates from the osmotic aggregates. Similar extensions were never observed in aging aggregates. (*D*) *vha-6p::Q44-YFP* animals were grown from the L1 stage on either 50 or 200 mM NaCl. Young adults from either group were then transferred to NGM plates with the indicated NaCl concentration, and the percentage of animals with aggregates was quantified after 4 h. $n \geq 40$ animals per condition. Data shown are mean ± SD. (*E*) Representative images of young adult animals expressing the indicated polyQ-length protein exposed to either 50 or 500 mM NaCl for 4 h. (Scale bars, 100 μm.) (*F*) Quantification of aggregation properties over time following exposure to 500 mM NaCl. $n > 40$ animals per genotype. Data shown are mean ± SD.

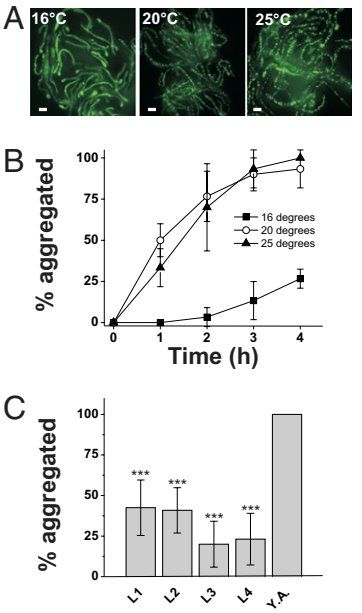


**Fig. 2.** Osmotically induced polyQ aggregation is influenced by growth temperature and age. (*A*) Representative image of worms grown at the indicated temperature and then exposed to 500 mM NaCl for 4 h as first-day adults. (Scale bars, 100 μm.) (*B*) Percentage of aggregated young adult animals that express intestinal Q44-YFP following exposure to 500 mM NaCl after growth at the indicated temperature. $n > 40$ animals for each genotype. Data shown are mean ± SD. (*C*) Percentage of aggregated animals following a 4-h exposure to 500 mM NaCl at the indicated developmental age. Y.A., young adult. $n > 40$ animals for each genotype. Data shown are mean ± SD. $^{***}P < 0.001$.

transition of Q44 proteins from a soluble to an aggregated form (Fig. 1 *A* and *B*). Aggregation could also be induced by exposure to either hyperosmotic sucrose or sorbitol (Fig. 1*A*), suggesting that aggregation is driven by osmotic and not ionic mechanisms. Aggregates formed in young adult animals grown at 20 or 25 °C but not in young adult animals of the same age grown at 16 °C (Fig. 2 *A* and *B*), suggesting that osmotically induced aggregation is not simply a stochastic response to alterations in cytoplasmic solute levels or cell volume. Aggregation was also significantly reduced in larval animals compared with young adults (Fig. 2*C*), suggesting that the effect of stress on aggregation is age-dependent. Aggregation was dependent on the level of hyperosmolarity (Fig. 1*D*; $EC_{50}$ = 484 ± 19 mM NaCl for animals grown at 50 mM NaCl), and the aggregation threshold could be shifted to higher concentrations following adaptation to hypertonicity (Fig. 1*D*; $EC_{50}$ for animals grown at 200 mM NaCl = 662 ± 28 mM NaCl). Acquisition of adaptation was detected after a 1-h exposure to 200 mM NaCl and appeared maximal by 3 h (Fig. S1*A*). Loss of adaptation was detected after 1 h of exposure to isotonic conditions and continued to diminish over 4 h (Fig. S1*B*). Osmotically induced aggregation was not a property of all polyQ proteins, and was only observed with Q repeats of >40 (Fig. 1*F*). Exposure to either heat shock (37 °C) or oxidative stress (200 μM juglone) failed to induce the aggregation of the polyQ reporter within the intestine (Fig. 1*A*). Taken together, these data show that hyperosmotic stress, but not other stressors, induces rapid Q length-dependent protein aggregation in *C. elegans* intestinal epithelial cells.

**Osmotically Induced PolyQ Aggregates Are Distinct from Aging-Induced Aggregates.** Osmotically induced polyQ aggregates appeared distinct in both number and morphology from aggregates that formed in aged animals. For example, aging induced the formation of small numbers of aggregates within the cytoplasm (18) (Fig. 1*C*). In contrast, exposure to hyperosmotic stress induced the formation of a large number of small, fibrillar cytoplasmic aggregates (Fig. 1*C*). These foci could form either as large aging-like aggregates that become fragmented over time or as small, individual aggregates that are distinct from aging-type aggregates. Time-lapse imaging of Q44-YFP animals exposed to 500 mM NaCl (Movie S1) revealed that large aging-like aggregates never form during exposure to hyperosmotic stress. Instead, hundreds of smaller aggregates appear to arise simultaneously. Therefore, osmotically induced aggregates do not appear to form through fragmentation of

large aggregates but rather through a large number of individual seeding events.

Osmotically induced aggregates also appeared morphologically distinct from aging-induced aggregates. Whereas age-induced aggregates exhibited a compact and spherical morphology (Fig. 1*C*, *Left*), osmotically induced aggregates exhibited irregular and fibrillar characteristics (Fig. 1*C*, *Right*). Osmotic Q44-YFP aggregates did not appear to be intermediates in the formation of aging aggregates, as their morphology remained stable over days. To determine whether the osmotically induced foci were in fact aggregates, we analyzed their biophysical properties using the fluorescence recovery after photobleaching (FRAP) technique (11, 12, 30, 31) (Fig. 3*A*). Consistent with their soluble and freely diffusible nature, nonaggregated, cytoplasmic Q44-YFP exhibited rapid fluorescent recovery following photobleaching (Fig. 3*C*). However, aging-induced Q44-YFP aggregates exhibited little recovery (Fig. 3*C*). Like age-induced Q44-YFP aggregates, osmotically induced Q44-YFP foci also failed to recover to wild-type levels, although the extent of fluorescent recovery was significantly larger than the recovery observed in age-induced aggregates, suggesting that osmotically induced aggregates contain a larger pool of exchangeable protein (Fig. 3*C*). The differences in aggregate morphology and diffusion

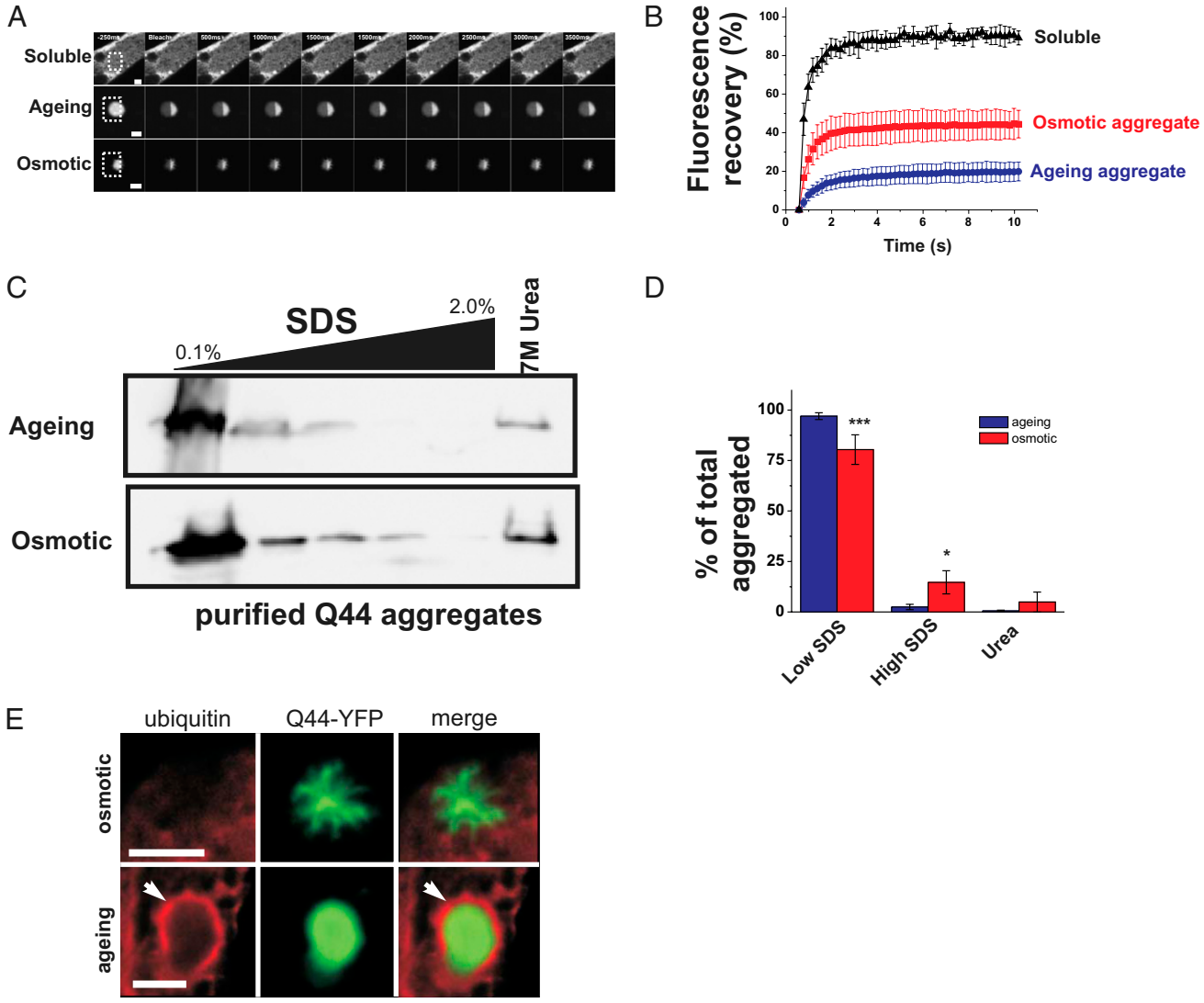


**Fig. 3.** Aging-induced polyQ aggregates can be differentiated from osmotically induced polyQ aggregates. (*A*) Time-series confocal images of soluble Q44-YFP (*Top*), aging-induced aggregates (*Middle*), and osmotically induced aggregates (*Bottom*). Boxed regions indicate FRAP areas. (Scale bars, 5 μm.) (*B*) Fluorescence quantification of bleached area in the indicated form of the Q44-YFP protein. Data shown are mean ± SD (soluble, $n = 6$; aging, $n = 8$; osmotic, $n = 10$). (*C*) Western blot (anti-GFP antibody) of aging and osmotically aggregated Q44-YFP protein extracted with increasing levels of SDS and urea buffers. Aggregates were isolated by lysis of worms in RIPA buffer followed by high-speed ultracentrifugation. The high-speed pellet was then extracted with RIPA buffer containing the indicated SDS levels (for more details, see *SI Materials and Methods*). The gel is representative of one of four independent experiments. (*D*) Quantification of the relative fraction of aggregated Q44-YFP protein extracted with low-SDS RIPA buffers (sum of 0.1% and 0.5% fractions), high-SDS RIPA buffers [sum of 1.0%, 1.5%, 2.0% (wt/vol) fractions], and 7 M urea buffer, expressed as a percentage of the total aggregated material (sum of the material in all lanes). Data shown are the mean ± SD from four independent experiments. $^{*}P < 0.05$, $^{***}P < 0.001$, one-way ANOVA with Tukey's post hoc test. (*E*) Deconvolved immunofluorescence image of osmotic Q44-YFP aggregate (*Upper*, 24 h poststress exposure) or aging Q44-YFP aggregate (*Lower*, 4-d-old animal) stained with a ubiquitin-specific antibody. Arrows indicate the ubiquitin-stained surface of an aging aggregate. Osmotic aggregates failed to stain with ubiquitin antibodies after they were aged for 4 d, suggesting that prolonged incubation times do not result in ubiquitination of osmotic aggregates. (Scale bars, 5 μm.)

rates suggest that aging and osmotic polyQ aggregates may represent structurally distinct aggregate species.

To further test this hypothesis, we compared aging and osmotic polyQ aggregates using biochemical and cell biological approaches. We isolated both aggregate species from *C. elegans* and examined their chemical sensitivity to SDS extraction. Sequential extraction of purified aging aggregates (from day 4 adults) or osmotic aggregates (from day 1 adults exposed to 500 mM NaCl for 4 h) with increasing concentrations of SDS showed that osmotically induced aggregates were significantly more resistant to SDS extraction than aging-induced aggregates (Fig. 3 *B* and *D*), suggesting differences in structure between the two aggregate species. We hypothesized that such differences in aggregate structure may cause cells to recognize each aggregate species in different ways, possibly via differences in their association with aggregate-interacting proteins (AIPs). Ubiquitin is a well-known AIP that associates with aging polyQ aggregates in mammalian cells (32). Using a ubiquitin-specific antibody, we found that age-induced polyQ aggregates were associated with ubiquitin in *C. elegans* intestinal cells (46/51 aggregates; 90.1%). However, osmotic aggregates showed no evidence of association with ubiquitin (0/74 aggregates; $P < 0.001$, Fisher's exact test; Fig. 3*E*). Taken together, these data demonstrate that osmotically induced Q44 foci exhibit the properties of aggregates but that they differ from age-induced aggregates in their morphological, biophysical, biochemical, and cell biological characteristics.

**Exposure of Mammalian Cells to Hyperosmotic Stress Induces Rapid Cytoplasmic Protein Aggregation.** To determine whether the formation of polyQ protein aggregates by osmotic stress is specific to *C. elegans* or also occurs in other species, we expressed a previously described polyQ protein containing the first exon of the Huntington gene (HTT-Q19-CFP or HTT-Q72-YFP) in mammalian HEK293 cells (14). Under isotonic conditions, cells expressing GFP alone or HTT-Q19-CFP exhibit diffuse cytoplasmic and nuclear staining, whereas cells expressing HTT-Q72-YFP exhibit nuclear aggregation (primarily a single large nuclear aggregate in each cell) with some diffuse cytoplasmic staining (Fig. 4 *A* and *C*). Following a 3-h exposure to 200 mM NaCl, HTT-Q72-YFP–expressing cells, but not GFP or HTT-Q19-CFP–expressing cells, exhibited an increase in large nuclear aggregates as well as the appearance of small, irregularly shaped aggregates, which were not present in unstressed cells (Fig. 4 *B* and *D*). As in *C. elegans*, the formation of osmotically induced aggregates in HEK293 cells was osmotic rather than ionic in nature, because aggregates were induced using the nonionic solute sorbitol (Fig. S2). Whereas the large HTT-Q72-YFP aggregates colocalized with nuclear Hoechst dye staining as previously reported (14), the small osmotic stress-induced aggregates did not colocalize with Hoechst dye, indicating that they were cytoplasmic in nature (Fig. S3). Of several tested stressors, only osmotic stress induced the formation of cytoplasmic protein aggregates (Fig. S4). Cells with cytoplasmic aggregates were alive, as assessed by their ability to exclude the vital dye Sytox (Fig. S5). As in worms, we were able to detect ubiquitin association with dense aging-type aggregates (11/247 aggregates; 4.4%), but we never observed an association between ubiquitin and osmotically induced aggregates (0/118 aggregates; $P = 0.0191$, Fisher's exact test). The significant difference in the fraction of ubiquitin-positive aging-type aggregates between *C. elegans* and HEK cells is likely due to constitutive cell division present in HEK cells, which does not occur in postmitotic *C. elegans* intestinal cells. Overall, these data demonstrate that osmotically induced cytoplasmic polyQ protein aggregation also occurs in mammalian cell culture and that such aggregates are morphologically and cell biologically distinct from previously described aging-type polyQ aggregates.

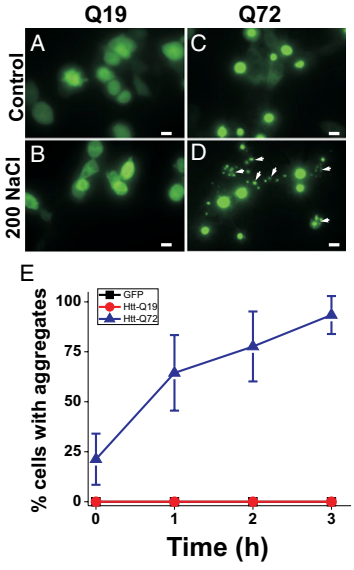


**Fig. 4.** Osmotic stress-induced Q-length–dependent protein aggregation in HEK293 cells. Nonthreshold Q19 (*A* and *B*) or threshold Q72 (*C* and *D*) exposed to either isotonic PBS (*A* and *C*) or PBS + 200 mM NaCl (*B* and *D*) for 3 h. Arrows point to cytoplasmic osmotically induced polyQ aggregates. (Scale bars, 10 μm.) (*E*) Quantification of the percentage of cells with aggregates (mean ± SD) over 3 h of exposure to 200 mM NaCl. $n = 10–12$ cell fields per genotype per time point.

**Genetic Activation of the Osmotic Stress Response, but Not Insulin-Like Growth Factor Signaling, Confers Specific Protection Against Stress-Induced Aggregation.** Reduced signaling of the insulin/insulin-like growth factor (IGF) pathway protects *C. elegans* from several environmental stressors, including hyperosmotic stress (25, 27, 33). Protection against hyperosmotic stress depends on the activity of several protein chaperones that are up-regulated by the FOXO transcription factor *daf-16* (33). Such protection could occur either by preventing the formation of osmotically induced protein aggregates or by mitigating the physiological effects of such aggregates. To distinguish between these possibilities, we crossed the *daf-2(e1370)* mutant, which causes constitutive FOXO signaling and protects against hyperosmotic stress, into the threshold-length polyQ lines. We confirmed that in these polyQ backgrounds, *daf-2(e1370)* still activates DAF-16/FOXO signaling (i.e., formation of dauer larvae at the restrictive temperature) and provides protection against hyperosmotic stress [increased 24-h survival on 500 mM NaCl (33)]. The *daf-2(e1370)* mutation had no effect on osmotically induced polyQ aggregate formation in muscle (Fig. S7), and caused only a modest delay in the kinetics of osmotically induced aggregate formation in the intestine (Fig. 5 *A* and *B*). By contrast, *daf-2* mutants exhibit a substantial reduction in the formation of intestinal age-induced polyQ aggregates (Fig. S6). Therefore, a reduction in IGF signaling strongly attenuates the formation of aging-induced Q44-YFP aggregates but has substantially weaker effects on the formation of osmotically induced Q44-YFP aggregates.

Another signaling pathway that protects *C. elegans* from hyperosmotic stress is the osmotic stress resistance (Osr) pathway (17, 34–36). Previously, we and others showed that Osr mutants, such as *osm-7* and *osm-8*, constitutively activate an osmosensitive gene expression program and have high levels of the organic osmolyte glycerol (17, 28, 35). However, these mutants do not exhibit transcriptional patterns characteristic of the response to other stressors such as heat shock or oxidative stress (17), and in the case of the *osm-8* mutant are resistant to lethal levels of hyperosmotic stress but not heat shock or oxidative stress (34). We crossed the Osr mutants *osm-7(n1515)* and *osm-8(n1518)* into the *vha-6p::Q44-YFP* background and found that osmotically induced aggregation was strongly attenuated (Fig. 5 *C* and *D*). The protective effect of the Osr mutants is not

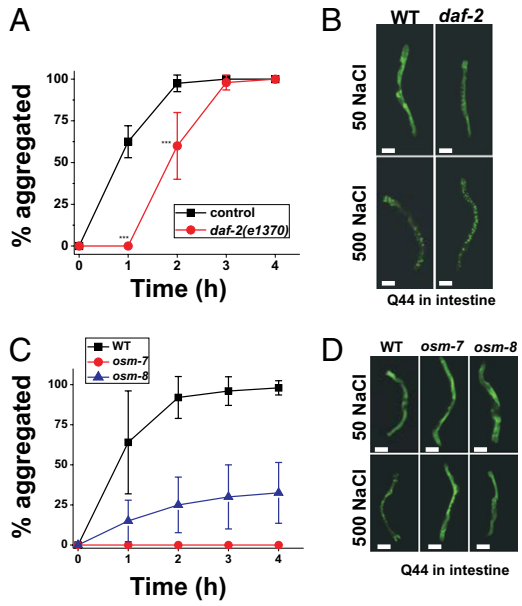


**Fig. 5.** Genetic activation of the osmotic stress resistance-signaling pathway but not the insulin-like growth factor–signaling pathway prevents the formation of osmotically induced Q44-YFP protein aggregates. (*A*) Percentage of aggregated young adult animals that express intestinal Q44-YFP following exposure to 500 mM NaCl for wild type and *daf-2(e1370)*. $n \geq 40$ animals for each genotype. ***$P < 0.001$ vs. control. (*B*) Representative images of wild type and *daf-2(e1370)* animals expressing intestinal Q44-YFP following 4 h of exposure to either 50 or 500 mM NaCl. (Scale bars, 100 μm.) (*C*) Percentage of aggregated young adult animals that express intestinal Q44-YFP following exposure to 500 mM NaCl for wild type, *osm-7(n1515)*, and *osm-8 (n1518)*. $n \geq 40$ animals for each genotype. (*D*) Representative images of wild type, *osm-7(n1515)*, and *osm-8(n1518)* animals expressing intestinal Q44-YFP after 4 h of exposure to either 50 or 500 mM NaCl. (Scale bars, 100 μm.)

limited to the intestine, because the Osr mutants also protect muscle cells against osmotically induced aggregation (Fig. S7). We also found that the Osr mutants *osm-7* and *osm-8* provided significant protection against aging-induced polyQ aggregation in the intestine, although such protection was significantly weaker than that provided by *daf-2(e1370)*, which does not contain elevated levels of glycerol (33) (Fig. S6). Together, these data show that genetic and physiological activation of the osmotic stress-response pathway, but not the IGF-signaling pathway, attenuates stress-induced polyQ aggregation in multiple tissues. Furthermore, the Osr pathway provides weak but significant protection against aging-induced polyQ aggregation.

## Discussion

Aging and the environment are thought to strongly influence protein-folding processes, but in vivo comparisons between the effects of aging and the environment on protein folding have so far not been made. By taking advantage of a metastable polyQ-YFP reporter of protein folding in both *C. elegans* and mammalian cells, we gained insights into these processes in several ways. First, different environmental stressors do not all cause the same type of polyQ misfolding but rather evoke specific types of protein damage. Second, osmotic stress-induced polyQ aggregation is a consequence of osmotic stress in both *C. elegans* and mammalian cells. Third, osmotic stress-induced polyQ aggregates are distinct from aging-induced polyQ aggregates, based on multiple criteria. Finally, two pathways that promote survival of *C. elegans* in hyperosmotic environments, the IGF pathway and the Osr pathway, have different effects on stress-induced polyQ protein aggregation and likely protect *C. elegans* from environmental stress through distinct mechanisms. Together, these data provide insights into the specific effects of stress and aging on protein folding in vivo.

Although aging and osmotic stress both cause polyQ aggregation, our findings reveal differences in the nature of the aggregates that form under these conditions. Before our studies, these differences were not appreciated. Several pieces of data support the conclusion that osmotically induced polyQ aggregates are intrinsically different from aging-induced polyQ aggregates, although we note that our data do not allow us to resolve potential differences in the structure of the monomeric Q44-YFP protein. First, increased FRAP recovery and resistance to SDS extraction indicate that osmotic aggregates contain different underlying aggregate structure from aging aggregates. Second, the lack of ubiquitin association with osmotically induced polyQ aggregates suggests the two aggregate species exhibit distinct protein interactions within the cell. Finally, Osr-regulated stress pathways, but not *daf-2*–regulated aging pathways, protect against stress-induced polyQ aggregation. The differential response of stress-induced aggregates to these two signaling pathways suggests that different mechanisms protect cells against stress and aging aggregates. However, it is important to consider that the polyQ proteins are nonnative substrates. In the future, it will be important to identify native cellular proteins that aggregate in response to stress and aging in different tissues, compare their underlying aggregate structures and interacting proteins, and determine whether such native protein aggregates respond differently to activation of stress- and aging-signaling pathways. Toward these goals, recent studies identified native proteins that aggregate with age (23), whereas other studies showed that yet to be identified native proteins aggregate in response to osmotic stress (4).

Genetic studies have shown an important role for both the IGF and Osr pathways in mediating protection against hyperosmotic stress (33, 36). The Osr mutants exert their effects through constitutive activation of osmosensitive signaling and organic osmolyte production (17, 34). Previous data suggested that exogenous administration of the nonnative organic osmolyte trehalose inhibits protein aggregation and pathophysiology in diseases of protein misfolding (37–39). However, our data show that genetic activation of a native osmolyte accumulation-signaling pathway in animals can also protect against protein aggregation. Although our time course studies reveal a tight correlation between acquisition and loss of protection via adaptation (Fig. S1) and the gain and loss of the organic osmolyte glycerol (40), it is currently unclear whether this effect is mediated by the increased production of osmolytes or through other mechanisms activated by the Osr and osmotic adaptation pathway(s). A better understanding of these mechanisms might be leveraged to delay or prevent protein aggregation-based disease phenotypes in mammals.

Whereas Osr mutants activate native osmotic adaptation pathways, IGF mutants do not activate these pathways. Instead, IGF-mediated protection against hyperosmotic stress requires the function of several heat shock proteins (33), suggesting that IGF signaling prevents and/or protects against the consequences of protein misfolding. Currently, there are data supporting both of these possibilities. For example, our data suggest that for polyQ proteins, IGF signaling does not prevent stress-induced aggregation. Previous data demonstrating that IGF signaling protects *C. elegans* from Aβ toxicity without reducing aggregation supports such a possibility (41). However, *daf-2* might not protect against stress-induced polyQ protein aggregation simply because it occurs rapidly (compared with aging-induced aggregate formation, which occurs over a time course of days), and *daf-2* up-regulated processes (i.e., autophagy, chaperone proteins, protein turnover, etc.) act too slowly to prevent rapidly forming aggregates. Arguing against this possibility is a recent study demonstrating that *daf-2* mutants inhibit the formation of as yet unidentified detergent-insoluble protein species induced by osmotic stress (4). Therefore, IGF signaling could have dual roles in protecting cells against proteotoxicity (41).

In conclusion, using a polyQ protein as a sensor of cellular protein folding, we have shown that environmental stress and aging place different protein-folding burdens on both *C. elegans* and mammalian cells. Moreover, we show that the same cellular protein can adopt distinct aggregation states depending on whether it misfolds in the context of an environmental stressor or aging. Such distinct aggregation states may provide a sensor that allows cells to distinguish between different proteotoxic stressors and activate physiological responses through appropriately tuned signaling pathways that detect specific forms of protein damage.

## Materials and Methods

**Stress Exposures.** Young adult *C. elegans* were raised on standard nematode growth media plates at 20 °C (unless noted otherwise) and exposed to the indicated stressors on plates with *Escherichia coli* strain OP50 as previously described (17, 34). All oxidative stress compounds were included in the growth agar and, in the case of juglone, poured immediately before use. Before assays, worms were raised on standard NGM plates fed OP50 at 20 °C (unless noted otherwise). All stress assays were performed on day 1 (24 h post-larval stage 4) animals. At this time point, *drls20* animals do not contain age-induced polyQ aggregates. "Aging" assays used animals on day 3–4 of adulthood, except for animals in Fig. S6, which used animals on day 7 of adulthood. All chemicals were obtained from Sigma.

**Statistics.** Aggregation data and Western blot quantification were analyzed using either the Student's *t* test or ANOVA, as implemented in GraphPad Prism or Microsoft Excel. *P* values <0.05 were taken to indicate significance.

Additional details of experimental procedures are provided in *SI Materials and Methods*.

**ACKNOWLEDGMENTS.** We thank Danielle Garsin (University of Texas, Houston) for providing the *vha-6p::polyQ* strains and vectors; Robert Baloh (Washington University School of Medicine) for providing the polyQ HEK cell expression constructs; and David Raizen, Jessica Tanis, and the anonymous reviewers for constructive comments on the manuscript. Some nematode strains used in this work were provided by the *Caenorhabditis* Genetics Center, which is funded by the National Institutes of Health (NIH) National Center for Research Resources. This work was supported by NIH Grants R01AA017580 (to T.L.) and R01NS052325 and R21NS064232 (to R.G.K.).

1. Nakamura T, Lipton SA (2007) Molecular mechanisms of nitrosative stress-mediated protein misfolding in neurodegenerative diseases. *Cell Mol Life Sci* 64:1609–1620.
2. Scandalios JG (2005) Oxidative stress: Molecular perception and transduction of signals triggering antioxidant gene defenses. *Braz J Med Biol Res* 38:995–1014.
3. Grune T, Jung T, Merker K, Davies KJ (2004) Decreased proteolysis caused by protein aggregates, inclusion bodies, plaques, lipofuscin, ceroid, and 'aggresomes' during oxidative stress, aging, and disease. *Int J Biochem Cell Biol* 36:2519–2530.
4. Burkewitz K, Choe K, Strange K (2011) Hypertonic stress induces rapid and widespread protein damage in *C. elegans*. *Am J Physiol Cell Physiol* 301:C566–C576.
5. Choe KP, Strange K (2008) Genome-wide RNAi screen and in vivo protein aggregation reporters identify degradation of damaged proteins as an essential hypertonic stress response. *Am J Physiol Cell Physiol* 295:C1488–C1498.
6. Voellmy R (1994) Transduction of the stress signal and mechanisms of transcriptional regulation of heat shock/stress protein gene expression in higher eukaryotes. *Crit Rev Eukaryot Gene Expr* 4:357–401.
7. Yancey PH, Clark ME, Hand SC, Bowlus RD, Somero GN (1982) Living with water stress: Evolution of osmolyte systems. *Science* 217:1214–1222.
8. van Dellen A, Grote HE, Hannan AJ (2005) Gene-environment interactions, neuronal dysfunction and pathological plasticity in Huntington's disease. *Clin Exp Pharmacol Physiol* 32:1007–1019.
9. Gusella JF, MacDonald ME (2006) Huntington's disease: Seeing the pathogenic process through a genetic lens. *Trends Biochem Sci* 31:533–540.
10. Ignatova Z, Gierasch LM (2006) Extended polyglutamine tracts cause aggregation and structural perturbation of an adjacent β barrel protein. *J Biol Chem* 281:12959–12967.
11. Brignull HR, Moore FE, Tang SJ, Morimoto RI (2006) Polyglutamine proteins at the pathogenic threshold display neuron-specific aggregation in a pan-neuronal *Caenorhabditis elegans* model. *J Neurosci* 26:7597–7606.
12. Nollen EA, et al. (2004) Genome-wide RNA interference screen identifies previously undescribed regulators of polyglutamine aggregation. *Proc Natl Acad Sci USA* 101: 6403–6408.
13. Morley JF, Brignull HR, Weyers JJ, Morimoto RI (2002) The threshold for polyglutamine-expansion protein aggregation and cellular toxicity is dynamic and influenced by aging in *Caenorhabditis elegans*. *Proc Natl Acad Sci USA* 99:10417–10422.
14. Fuentealba RA, et al. (2010) Interaction with polyglutamine aggregates reveals a Q/N-rich domain in TDP-43. *J Biol Chem* 285:26304–26314.
15. GuhaThakurta D, et al. (2002) Identification of a novel *cis*-regulatory element involved in the heat shock response in *Caenorhabditis elegans* using microarray gene expression and computational methods. *Genome Res* 12:701–712.
16. Oliveira RP, et al. (2009) Condition-adapted stress and longevity gene regulation by *Caenorhabditis elegans* SKN-1/Nrf. *Aging Cell* 8:524–541.
17. Rohlfing AK, Miteva Y, Hannenhalli S, Lamitina T (2010) Genetic and physiological activation of osmosensitive gene expression mimics transcriptional signatures of pathogen infection in *C. elegans*. *PLoS One* 5:e9010.
18. Mohri-Shiomi A, Garsin DA (2008) Insulin signaling and the heat shock response modulate protein homeostasis in the *Caenorhabditis elegans* intestine during infection. *J Biol Chem* 283(1):194–201.
19. Gidalevitz T, Krupinski T, Garcia S, Morimoto RI (2009) Destabilizing protein polymorphisms in the genetic background direct phenotypic expression of mutant SOD1 toxicity. *PLoS Genet* 5:e1000399.
20. Ben-Zvi A, Miller EA, Morimoto RI (2009) Collapse of proteostasis represents an early molecular event in *Caenorhabditis elegans* aging. *Proc Natl Acad Sci USA* 106: 14914–14919.
21. Gidalevitz T, Ben-Zvi A, Ho KH, Brignull HR, Morimoto RI (2006) Progressive disruption of cellular protein folding in models of polyglutamine diseases. *Science* 311: 1471–1474.
22. Hsu AL, Murphy CT, Kenyon C (2003) Regulation of aging and age-related disease by DAF-16 and heat-shock factor. *Science* 300:1142–1145.
23. David DC, et al. (2010) Widespread protein aggregation as an inherent part of aging in *C. elegans*. *PLoS Biol* 8:e1000450.
24. Muñoz MJ (2003) Longevity and heat stress regulation in *Caenorhabditis elegans*. *Mech Ageing Dev* 124(1):43–48.
25. Cypser JR, Johnson TE (2002) Multiple stressors in *Caenorhabditis elegans* induce stress hormesis and extended longevity. *J Gerontol A Biol Sci Med Sci* 57:B109–B114.
26. Henderson ST, Johnson TE (2001) daf-16 integrates developmental and environmental inputs to mediate aging in the nematode *Caenorhabditis elegans*. *Curr Biol* 11:1975–1980.
27. Lithgow GJ, White TM, Melov S, Johnson TE (1995) Thermotolerance and extended life-span conferred by single-gene mutations and induced by thermal stress. *Proc Natl Acad Sci USA* 92:7540–7544.
28. Lamitina T, Huang CG, Strange K (2006) Genome-wide RNAi screening identifies protein damage as a regulator of osmoprotective gene expression. *Proc Natl Acad Sci USA* 103:12173–12178.
29. Morley JF, Morimoto RI (2004) Regulation of longevity in *Caenorhabditis elegans* by heat shock factor and molecular chaperones. *Mol Biol Cell* 15:657–664.
30. Brignull HR, Morley JF, Garcia SM, Morimoto RI (2006) Modeling polyglutamine pathogenesis in *C. elegans*. *Methods Enzymol* 412:256–282.
31. Kim S, Nollen EA, Kitagawa K, Bindokas VP, Morimoto RI (2002) Polyglutamine protein aggregates are dynamic. *Nat Cell Biol* 4:826–831.
32. Chai Y, Koppenhafer SL, Shoesmith SJ, Perez MK, Paulson HL (1999) Evidence for proteasome involvement in polyglutamine disease: Localization to nuclear inclusions in SCA3/MJD and suppression of polyglutamine aggregation in vitro. *Hum Mol Genet* 8:673–682.
33. Lamitina ST, Strange K (2005) Transcriptional targets of DAF-16 insulin signaling pathway protect *C. elegans* from extreme hypertonic stress. *Am J Physiol Cell Physiol* 288:C467–C474.
34. Rohlfing AK, Miteva Y, Moronetti L, He L, Lamitina T (2011) The *Caenorhabditis elegans* mucin-like protein OSM-8 negatively regulates osmosensitive physiology via the transmembrane protein PTR-23. *PLoS Genet* 7:e1001267.
35. Wheeler JM, Thomas JH (2006) Identification of a novel gene family involved in osmotic stress response in *Caenorhabditis elegans*. *Genetics* 174:1327–1336.
36. Solomon A, et al. (2004) *Caenorhabditis elegans* OSR-1 regulates behavioral and physiological responses to hyperosmotic environments. *Genetics* 167(1):161–170.
37. Sarkar S, Davies JE, Huang Z, Tunnacliffe A, Rubinsztein DC (2007) Trehalose, a novel mTOR-independent autophagy enhancer, accelerates the clearance of mutant huntingtin and α-synuclein. *J Biol Chem* 282:5641–5652.
38. Davies JE, Sarkar S, Rubinsztein DC (2006) Trehalose reduces aggregate formation and delays pathology in a transgenic mouse model of oculopharyngeal muscular dystrophy. *Hum Mol Genet* 15(1):23–31.
39. Tanaka M, et al. (2004) Trehalose alleviates polyglutamine-mediated pathology in a mouse model of Huntington disease. *Nat Med* 10(2):148–154.
40. Lamitina ST, Morrison R, Moeckel GW, Strange K (2004) Adaptation of the nematode *Caenorhabditis elegans* to extreme osmotic stress. *Am J Physiol Cell Physiol* 286: C785–C791.
41. Cohen E, Bieschke J, Perciavalle RM, Kelly JW, Dillin A (2006) Opposing activities protect against age-onset proteotoxicity. *Science* 313:1604–1610.

# Supporting Information

## Moronetti Mazzeo et al. 10.1073/pnas.1108766109

### SI Materials and Methods

***Caenorhabditis elegans* Strains.** All strains were maintained at 16 °C, 20 °C, or 25 °C using standard culture methods and fed with *Escherichia coli* strain OP50 (1). The following mutants and alleles were used in this study: LGII: *osm-8(n1518)*, *age-1(hx546)*; *LGIII: osm-7(n1515)*, *daf-2(e1370)*, *drIs20 [vha-6p::Q44-YFP, rol-6 (su1006)]*; LGX: *osm-11(n1604)*. *drIs20* was constructed by UV mutagenesis-mediated integration of strain GF80 ($^{+/+}$*; dgEx80 [vha-6p::Q44-YFP; rol-6(su1006)]*) (2). Integration was carried out by exposing ~50 *dgEx80* L4 animals to 30,000 μJ/cm$^2$ generated from a UV cross-linker (Stratagene). After singling the progeny of ~500 F1 animals, an integrated line segregating 100% *rol-6* animals was isolated and outcrossed three times to wild-type animals to generate *drIs20 [Pvha-6::Q44-YFP;rol-6(su1006)]*, which was used in all subsequent studies. All double-mutant combinations were constructed using standard crossing strategies. Strain genotypes were verified by visible recessive phenotypes and DNA sequencing.

**Fluorescence Microscopy and Fluorescence Recovery After Photobleaching Analysis.** For all aggregation assays, worms were imaged on a fluorescence-equipped stereo dissecting microscope (Leica MZ16FA). Worms with ≥10 distinguishable aggregates, defined as fluorescent puncta that could be defined from adjacent/background fluorescence on all edges, were considered aggregated animals (2). For aggregate morphology and time-lapse imaging experiments, levamisole (1 mM)-anesthetized animals were imaged on thin agarose pads containing the indicated levels of NaCl using a fluorescence inverted microscope (Leica DMI4000B) and digital camera (Leica DFC340Fx). Deconvolution of Z-stacked (0.2-μm step size) images was carried out in Leica image analysis software (advanced fluorescence 6000 software). For fluorescence recovery after photobleaching analysis, animals were imaged using a confocal microscope (Zeiss LSM510) with a 40×/1.2 N.A. water-immersion lens and bleached with five scans from a 488-nm laser at 100% power. Images (128 × 128 pixels) were collected every 250 ms after bleaching. The kinetics and time constants of recovery were calculated by fitting the data with the Hill function in OriginLab software. *C. elegans* immunohistochemistry was carried out on manually dissected intestines. Briefly, intestines were released from *drIs20* animals by manual dissection in 100 mM $K_2HPO_4$ and then fixed for 1 h at 4 °C in 100 mM $K_2HPO_4$ + 3% (vol/vol) paraformaldehyde (EM Biosciences). Fixed worms were washed five times in BT buffer (20 mM $H_3BO_3$, 10 mM NaOH, 0.5% Triton X-100), permeabilized for 1 h at 4 °C in BTB buffer [BT + 2% (vol/vol) β-mercaptoethanol], and blocked for 1 h at 4 °C in Aba buffer (1× PBS, 0.5% BSA, 0.5% Triton X-100). Samples were incubated overnight at 4 °C in anti-ubiquitin antibody diluted in Aba buffer (1:100 dilution; Dako), washed five times in Aba buffer, and then incubated for 2 h at 4 °C in a goat anti-rabbit Alexa 594 secondary antibody (1:1,000 dilution; Molecular Probes). After being washed five times in Aba buffer, samples were mounted in ProLong antifade (Invitrogen) reagent for imaging.

**PolyQ Protein Biochemistry.** To isolate osmotic aggregates, synchronized *drIs20* young adults (24 h post-L4 stage) were exposed to 500 mM NaCl NGM plates for 4 h to induce the formation of osmotic aggregates. For aging aggregates, young adult animals were aged on NGM plates containing fluorodeoxyuridine for 4 d after the L4 stage. Aged and osmotically stressed animals were processed in parallel using identical solutions and conditions. Specifically, the animals were rinsed from the plates with M9 solution and washed twice. One hundred microliters of washed pelleted worms were added to 500 μL of RIPA buffer [150 mM NaCl, 50 mM Tris·HCl (pH 7.5), 1 mM EGTA, 5 mM EDTA, 1% Nonidet P-40, 0.5% sodium deoxycholate, 0.1% SDS, Roche Complete Protease Inhibitor (0.1%), 0.5 mM PMSF] and were sonicated on ice (15 cycles, 30% power, 2-s pulse, 5-s rest; Branson Ultrasonics sonicator). Following sonication, the homogenate was subjected to a low-speed spin (400 × *g*, 5 min). The low-speed supernatant (500 μL) was then subjected to ultracentrifugation (100,000 × *g*, 30 min). The supernatant was removed and the pellet was resuspended in 500 μL of RIPA buffer + 0.1% SDS and sonicated on ice (1 cycle, 20% power, 2-s pulse). This extraction process was repeated for RIPA buffer + 0.5%, 1.0%, 1.5%, and 2.0% (wt/vol) SDS. The pellet from the 2% SDS extraction was then solubilized in 100 μL of urea buffer [30 mM Tris·HCl, 7 M urea, 2 M thiourea, 4% (wt/vol) CHAPS, 0.5 mM PMSF, Roche Complete Protease Inhibitor (0.1%)]. Ten microliters of each fraction (2% of the total fraction, except for the urea fraction, which was 10% of the total fraction) was added to 10 μL of 2× SDS sample buffer and then loaded onto a 10% (wt/vol) SDS/PAGE gel. Proteins were transferred onto nitrocellulose and then probed with a monoclonal anti-GFP antibody (1:1,000; Roche), which was detected using enhanced chemiluminescence. Band intensity was quantified using gel analysis routines in ImageJ (National Institutes of Health). The total amount of protein present in each sample was calculated and the amount of protein in each sample was calculated as a percentage of the total. The extraction and quantification procedure was repeated on four separate occasions with independently isolated samples.

**HEK Cell Experiments.** HEK293 cells were grown in Dulbecco's minimal essential media (Gibco) with 10% (vol/vol) heat-inactivated FBS (Gibco) and penicillin/streptomycin on laminin/polylysine-coated glass coverslips. Plasmids were transfected into cells using Lipofectamine 2000 (Invitrogen) according to the manufacturer's recommendations. One day after transfection, the cells were placed into either isotonic or hypertonic PBS and kept at 37 °C for up to 3 h. For heat-stress experiments, cells were incubated at 42 °C for 3 h. For oxidative stress, cells were incubated in PBS containing the indicated amounts of paraquat, EtOH, sorbitol, sucrose, or NaCl for 3 h. Antibody staining was carried out as previously described (3) using a polyclonal anti-ubiquitin antibody (1:100; Dako).


1. Brenner S (1974) The genetics of *Caenorhabditis elegans*. *Genetics* 77(1):71–94.
2. Mohri-Shiomi A, Garsin DA (2008) Insulin signaling and the heat shock response modulate protein homeostasis in the *Caenorhabditis elegans* intestine during infection. *J Biol Chem* 283(1):194–201.
3. Mojsilovic-Petrovic J, et al. (2009) FOXO3a is broadly neuroprotective in vitro and in vivo against insults implicated in motor neuron diseases. *J Neurosci* 29:8236–8247.

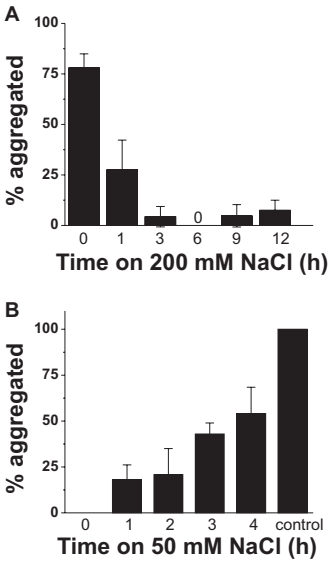


**Fig. S1.** Acquisition and loss of adaptation-mediated protection against osmotically induced polyQ aggregation. (*A*) Young adult (24 h post-L4 stage) *drIs20* hermaphrodites were grown their entire life on 50 mM NaCl NGM plates and then transferred to NGM plates containing 200 mM NaCl for the indicated periods. Animals were then placed on NGM plates containing 500 mM NaCl, and the percentage of animals containing aggregates was quantified after 4 h. Data shown are mean ± SD. $n = 4$ replicates, ≥40 animals per time point. (*B*) L4 stage *drIs20* hermaphrodites were transferred to NGM containing 200 mM NaCl for 24 h and then transferred to NGM plates containing 50 mM NaCl for the indicated periods. Animals were then placed on NGM plates containing 500 mM NaCl, and the percentage of animals containing aggregates was quantified after 4 h. Control, animals that were never exposed to 200 mM NaCl. Data shown are mean ± SD. $n = 4$ replicates, ≥40 animals per time point.

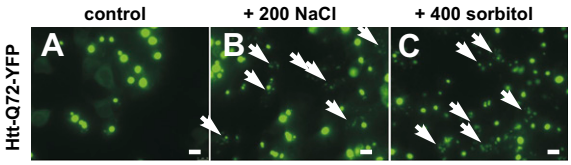


**Fig. S2.** Osmotically induced polyQ aggregation in mammalian cells is due to an osmotic effect. HEK293 cells transfected with HTT-Q72-YFP were exposed to control (*A*), 200 mM NaCl (*B*), or 400 mM sorbitol (*C*) for 3 h and then imaged. Arrows indicate cells containing cytoplasmic polyQ aggregates that are not observed in control cells. (Scale bars, 10 μm.)

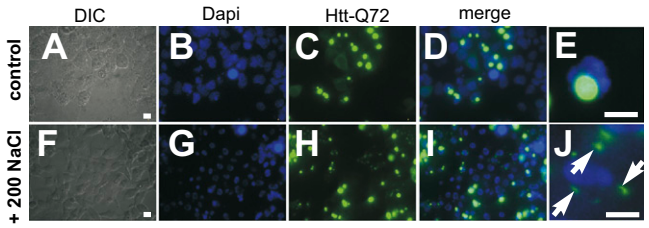


**Fig. S3.** Osmotically induced polyQ aggregates do not colocalize with nuclear DNA in HEK293 cells. HTT-Q72-YFP–expressing HEK cells exposed to control (*Upper*) or hypertonic 200 NaCl for 3 h (*Lower*). Arrows point to osmotically induced aggregates that do not colocalize with DAPI-stained nuclei. DIC, differential interference contrast. [Scale bars, 10 μm (*A–D* and *F–I*); 5 μm (*E* and *J*).]

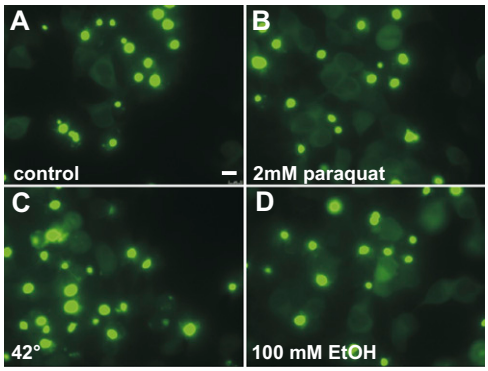


**Fig. S4.** Stress-induced polyQ aggregation does not occur in response to oxidative stress, heat stress, or ethanol stress in HEK293 cells. HTT-Q72-YFP–expressing HEK cells were exposed to the indicated stressors for 3 h and then imaged. (Scale bar, 10 μm.)

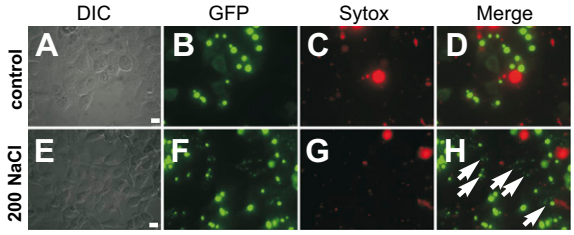


**Fig. S5.** Cells that contain osmotically induced polyQ aggregates are viable. HTT-Q72-YFP–expressing HEK293 cells exposed to isotonic PBS (*A–D*) or PBS + 200 mM NaCl (*E–H*) labeled with the vital dye Sytox Orange. Arrows point to cells with osmotically induced aggregates, which do not costain with Sytox dye. (Scale bars, 10 μm.)

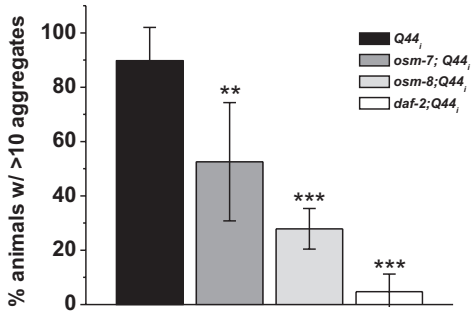


**Fig. S6.** Osmotic stress resistance mutants protect against aging-induced polyQ aggregation. Animals were aged for 7 d after the L4 stage, and the number of animals with fewer than 10 visible aggregates was counted. $n = 5$ trials, ≥10 worms per trial. Results are representative of two independent experiments. $^{**}P < 0.01$, $^{***}P < 0.001$.

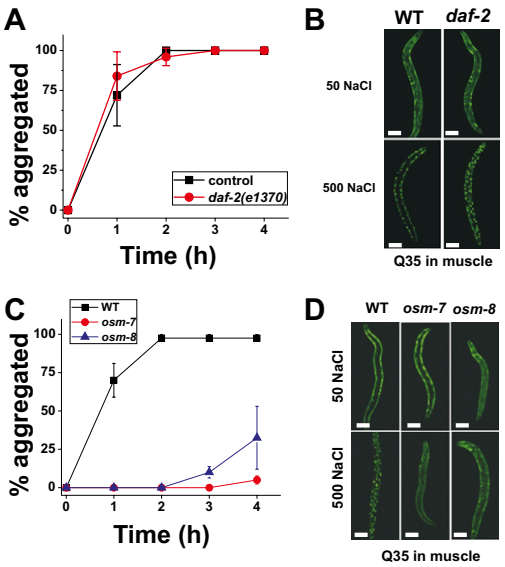


**Fig. S7.** Genetic activation of the osmotic stress-response pathway but not the insulin-like growth factor pathway blocks osmotically induced Q35-YFP aggregation in muscle. (*A*) Percentage of aggregated young adult animals that express muscle Q35-YFP following exposure to 500 mM NaCl for wild type and *daf-2(e1370)*. $n \geq 40$ animals for each genotype. (*B*) Representative images of wild-type or *daf-2(e1370)* animals expressing intestinal Q44-YFP following 4 h of exposure to either 50 or 500 mM NaCl. (Scale bars, 100 μm.) (*C*) Percentage of aggregated young adult animals that express muscle Q35-YFP following exposure to 500 mM NaCl for wild type, *osm-7(n1515)*, and *osm-8(n1518)*. $n \geq 40$ animals for each genotype. (*D*) Representative images of wild type, *osm-7(n1515)*, and *osm-8(n1518)* animals expressing Q35-YFP after 4 h of exposure to either 50 or 500 mM NaCl. (Scale bars, 100 μm.)

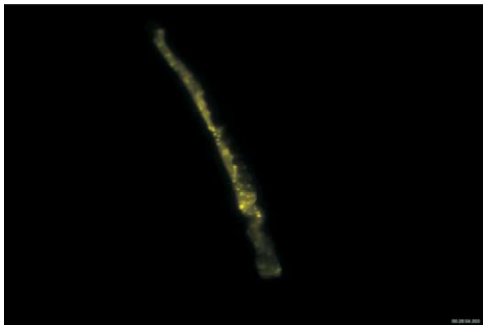

**Movie S1.** Osmotically induced aggregates are not derived from larger aging-type aggregates. Young adult hermaphrodite expressing Q44-YFP in the intestine was placed on a pad with 500 mM NaCl, and a Z stack of images was collected every 4 min. The movie represents the time series of collapsed Z sections.

Movie S1